Sequence-Specific Assignments in the ^1H NMR Spectrum of the Human Inflammatory Protein C5a

Erik R. P. Zuiderweg,* Karl W. Mollison, Jack Henkin, and George W. Carter

Pharmaceutical Discovery, Abbott Laboratories, Abbott Park, Illinois 60064

Received October 8, 1987

ABSTRACT: Full sequence-specific assignments for the ^1H NMR lines of the backbone protons of the human complement factor C5a are described and documented. The results were obtained by largely following the methodology developed by Wüthrich et al. [Wüthrich, K., Wider, G., Wagner, G., & Braun, W. (1982) *J. Mol. Biol. 155*, 311]. Assignments for the majority of the amino acid side chain protons were obtained by using a comparison of double- and triple-quantum-filtered two-dimensional correlated experiments together with the analysis of relayed coherence transfer spectra. The assignments provide the basis for the determination of the thus far unknown three-dimensional structure of C5a from nuclear Overhauser enhancement distance constraints.

The inflammatory protein C5a is cleaved from the N terminus of the α chain of the serum protein C5 during activation of the complement cascade (Mayer, 1979). Although C5a is not directly involved in antigen inactivation and metabolism, it possesses a range of biological activities that facilitate this process. C5a is the principal inflammatory protein derived from the complement system; this potent mediator stimulates the locomotion (chemokinesis) and recruitment (chemotaxis) of polymorphonuclear leukocytes to sites of inflammation and triggers these cells to release tissue-digesting enzymes and other damaging substances [for a review, see Hugli (1981)]. C5a has also been shown to augment antibody production, at least in vitro, by inducing release of monokines [reviewed in Weigle et al. (1983)]. The protein causes vasodilation and increases vascular permeability, induces the contraction of smooth muscle, and triggers the release of histamine from mast cells and basophilic leukocytes. Because of this broad range of biological properties, C5a has been implicated as a causative or aggravating agent in a variety of inflammatory and allergic diseases (Ward, 1970).

Compared to the number of studies of the biological functions of C5a, relatively few experiments have been carried out to investigate its structure. The sequence of C5a has been determined (Fernandez & Hugli, 1978), the secondary structure was characterized as predominantly α-helical from optical studies (Hugli, 1981), and the disulfide linakges between six of the seven cysteine residues were obtained from biochemical studies (Zimmerman & Vogt, 1984). No crystal structure is known for C5a, and no other nuclear magnetic resonance (NMR)[1] studies have been carried out on this protein to our knowledge. From comparative computer modeling, however, a full three-dimensional structure has been proposed for human C5a (Greer, 1985) on the basis of the crystal structure of the homologous complement factor C3a (Huber et al., 1980).

The assignments of the ^1H resonances of the NMR spectrum of C5a described in this paper form the basis for the determination of the solution structure of this relatively small protein (74 amino acids) from nuclear Overhauser effect (NOE) data. NMR structure determinations were recently described for several other small proteins [e.g., Braun et al. (1983), Zuiderweg et al. (1985), Williamson et al. (1985), Kline et al. (1986), Klevit and Waygood (1986), Cooke et al. (1987), and Clore et al. (1987)] and is rapidly becoming a well-established technique. Knowledge of the three-dimensional structure of the C5a should facilitate a variety of experiments such as site-directed mutagenesis and the selection and design of peptides to mimic the receptor-binding regions of the protein. The NMR studies were carried out by using recombinant C5a (75 residues) obtained as previously described (Mandecki et al., 1985). This protein, designated rC5a[Met0], is identical with human serum C5a except for the addition of an N-terminal methionine and the deletion of the carbohydrate chain at Asn-64. Careful biological studies showed no difference between human serum C5a and rC5a-[Met0] in receptor binding, stimulation of myeloperoxidase release, chemokinesis, or chemotaxis (Mollison et al., unpublished observations). Furthermore, the 1D proton NMR spectra of these species showed identical shifts for the aromatics and high-field-shifted methyl resonances (Zuiderweg, unpublished results), strongly indicating a similarly folded structure. The studies presented here give a full documentation of the sequence-specific resonance assignments for rC5a-[Met0], which were obtained by using the methodology originated in the group of Wüthrich (Wüthrich et al., 1982). In addition to the techniques originally used in that methodology, i.e., two-dimensional scalar correlated spectroscopy (COSY) (Aue et al., 1976) and two-dimensional nuclear Overhauser enhancement spectroscopy (NOESY) (Jeener et al., 1979), the present studies on C5a had to rely heavily on modern two-dimensional (2D) NMR methods such as relayed COSY (Wagner, 1983), double-quantum- and triple-quantum-filtered COSY (Rance et al., 1983; Muller et al., 1986), phase-sensitive COSY and NOESY (Muller & Ernst, 1979; States et al., 1982; Marion & Wüthrich, 1983), and to some extent 2D double-quantum spectroscopy (Braunschweiler et al., 1983; Wagner & Zuiderweg, 1983). As a result, all backbone protons were assigned and all proton resonances of 57 side chains could be identified. For the remaining side chains, exclusively the 18 Leu, Arg, Pro, and Lys residues, partial assignments were made.

[1] Abbreviations: NMR, nuclear magnetic resonance; NOE, nuclear Overhauser enhancement; 2D, two dimensional; COSY, 2D scalar correlated spectroscopy; NOESY, 2D nuclear Overhauser enhancement spectroscopy; DQF, double quantum filter; TQF, triple quantum filter.

0006-2960/88/0427-3568$01.50/0

Materials and Methods

The C5a protein used for this study was obtained from a synthetic gene (Mandecki et al., 1985) expressed in a protease-deficient strain of *E. coli* (Mandecki et al., 1986) that was grown under conditions giving high-level C5a expression (Mollison et al., 1987). The cells produced rC5a and rC5a[Met0] in an approximate weight ratio of 1:2. C5a was extracted from the cell paste, and the two C5a species were separated by high-performance liquid chromatography as described previously (Carter et al., 1986).

The NMR studies reported here were carried out with approximately 7 mM rC5a[Met0] (the more abundant species) in ^2H_2O or 90% H_2O/10% ^2H_2O solutions at pH 2.3 without any additional buffer. The NMR spectra were obtained at 500 MHz by use of a General Electric GN500 spectrometer equipped with a Nicolet 1280 computer and 293D pulse programmer. Phase-sensitive NOESY (States et al., 1982), COSY (Marion & Wüthrich, 1983), double- and triple-quantum-filtered COSY spectra (Rance et al., 1983; Muller et al., 1986), and absolute value relayed COSY spectra (Wagner, 1983) were collected by using the standard pulse sequences and phase programs. The NOESY and COSY spectra were acquired in the hypercomplex mode (Muller et al., 1979) with the radio frequency carrier placed in the center of the spectrum, whereas for the DQF and TQF spectra the carrier was placed at the high-field side of the spectrum, permitting single-phase detection in t_1. Suppression of the solvent resonance in the H_2O spectra was accomplished by continuous radio frequency saturation of the H_2O resonance except during t_1 and t_2 (Wider et al., 1984) using a time-shared pulse train from the continuous wave observe amplifier to obtain coherence with the observe pulses, thus suppressing ω_2 streaks (Zuiderweg et al., 1986). The raw data were transferred to a VAX 780 computer. The data were processed either on the VAX using software obtained from Dr. D. R. Hare or on a slave CSPI Minimap array processor using in-house-written software or with a combination of the two methods. For NOESY experiments care was taken to optimize the base line of the spectra by manipulating the intensity of the first points prior to both t_2 and t_1 Fourier transformations (Otting et al., 1986). The data were digitally filtered by using sine-bell window functions shifted in various amounts as described in the figure legends. The occurrence of t_2 ridges was minimized by either base-line correction of the ω_2 transformed slices with a fifth-order polynomial, automatic base-line correction of the rows of the frequency domain matrix, or both. The base plane of the spectrum was further improved by correcting the base lines of the ω_1 slices in the frequency domain matrix.

Results

The assignments for the NMR spectrum of rC5a[Met0] were obtained by applying the sequential assignment procedure for proteins originated in the group of Wüthrich (Wüthrich et al., 1982; Billeter et al., 1982), in which the resonance positions of the different amino acid protons are first sorted in sets of so-called spin systems by using scalar correlated 2D spectroscopy methods such as COSY, followed by a search for nuclear Overhauser effects (NOEs) between the backbone protons and backbone and C_β protons of residues adjacent in the protein primary structure using NOESY. The documentation of the assignments of rC5a[Met0] in this paper is presented by using the separation between spin-system assignment and sequential assignment as described in related papers on this subject. In practice, however, a substantial feedback between the different stages of the assignment procedure occurred. Moreover, after helicity was established for different regions of the protein from the qualitative comparison of the intensities of the sequential NOEs, medium-range NOEs $d_{\alpha N}(i, i + 3)$ and $d_{\alpha\beta}(i, i + 3)$ (Zuiderweg et al., 1983a; Williamson et al., 1984; Wüthrich et al., 1984) in these regions were exploited to confirm the assignments and to obtain missing assignments. Furthermore, COSY and NOESY spectra obtained from rC5a[Met0] in which the amide protons were partly exchanged for deuterons (Wagner, 1983b) provided an additional means to resolve the NH–C_αH intraresidue cross peaks and $d_{\alpha N}$ type connectivities in the crowded regions of the spectrum. Whenever ambiguities still existed, a comparison was made of spectra recorded at different temperatures and pH values. In addition, analysis was carried out of the spectra of the related rC5a species that differs by one amino acid at the N terminus of rC5a[Met0]. These variations in conditions and species provided a sufficient amount of chemical shift changes to resolve the chance degeneracies.

Identification of the Spin Systems. This section describes how the side-chain resonances of the different amino acid residues (the spin systems of nonexchangeable protons) were identified to belong to unique residues (Gly, Ala, Val, Ile, Leu, Thr) or to groups of residues (AMX spin systems Ser, Asp, Asn, Cys, His, Phe, Tyr; AMPTX spin systems Glu, Gln, Met; long side chain systems Arg, Lys, Pro). These identifications were mainly made prior to the sequence-specific resonance assignments; therefore, the position identifications used in this section and in the accompanying figures were not available at this stage (except for the unique Phe-51) and are used here only for purposes of easy reference.

The majority of the spin systems in rC5a[Met0] were identified from a combined analysis of COSY and relayed COSY in both H_2O and ^2H_2O and from double-quantum- and triple-quantum-filtered COSY in ^2H_2O recorded at 30 °C, at which conditions the line widths of rC5a[Met0] are sufficiently small (approximately 6 Hz) to allow sensitive coherence transfer experiments to be carried out. Two of the three glycine and all alanine systems were readily obtained from the comparison of TQF and DQF COSY experiments (Figure 1); the latter could be connected to the amide proton resonances by using relay in H_2O (Figure 2). All Val spin systems were identified from relay in ^2H_2O (Figure 3) and could be connected to the NH resonances by using relay in H_2O (Figure 2). The relay spectrum in ^2H_2O (figure 3) provided identifications of the $C_\alpha HC_\beta HC_\gamma H_3$ moieties of all Ile systems; the moieties $C_\gamma H_2C_\delta H_3$ were obtained from the TQF spectrum where the overlapping cross peaks of the linear spin systems of Val and Leu were eliminated (Muller et al., 1986) (Figure 1). For the residues I9, I48, and I65 the C_βH and one of the $C_\gamma H_2$ resonances could be connected in DQF COSY (Figure 1), while for Ile-6 the connectivity C_αH–$C_\gamma H_2$ could be established in relay (not shown). As a result, the spin-system moieties of the Ile spin systems could be connected (the remaining Ile-41 by elimination). The relay spectrum in H_2O provided sufficient resolution to identify the NH–C_αH–C_βH connectivities for Ile-9, -41, -48, and -65. The amide proton shift for Ile-6 could only be obtained at the end of the sequential assignment procedure. The three leucine spin systems could not be delineated at the outset of the resonance assignment procedure. All Thr systems were obtained from the DQF, TQF, and relay spectra (Figures 1 and 3); the amide proton connections could be established for Thr-33 and -52 by using relay in H_2O (e.g., Figure 2). The AMX spin systems C22, D24, C27, N29, N30, D31, C34, S42, C47, C54, C55,

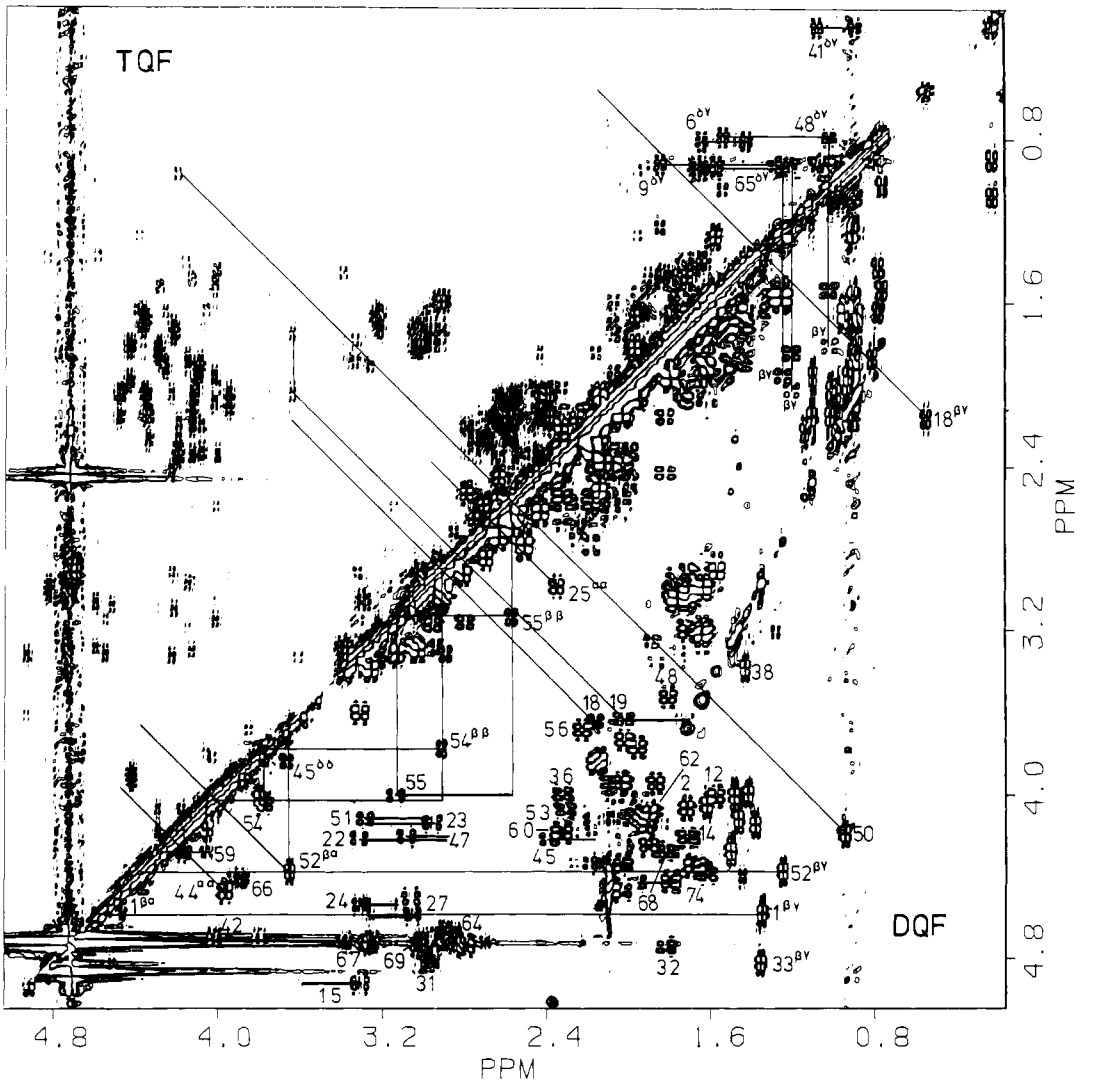

FIGURE 1: Combination contour plot of a 500-MHz triple-quantum-filtered (TQF) COSY spectrum (top triangle) and a double-quantum-filtered (DQF) COSY spectrum (bottom triangle) of rC5a[Met0] in ^2H_2O, pH 2.3, 30 °C. The spectra were collected with the carrier at the high-field end and processed by using a sine-bell shifted by 45° in t_2 and a unshifted sine bell in t_1. The digital resolution is 4.9 Hz/point in both dimensions. Positive and negative contour levels are shown. In the DQF spectrum the $C_\alpha H$–$C_\beta H$ connectivities are indicated by horizontal lines connecting both $C_\beta H$ resonances along the ω_2 axis (horizontal) with the $C_\alpha H$ resonances along the ω_1 axis unless indicated otherwise. In some cases the horizontal lines terminate at locations where no cross peaks are observed; these locations were deduced from the from $C_\beta H$–$C_\beta H$ cross peaks as indicated for Cys-54 and Cys-55 or from relay experiments (see Figure 3). The TQF spectrum was utilized to distinguish between two-spin or linear multispin systems and nonlinear multispin systems. Antidiagonal lines connecting corresponding positions in the DQF and TQF spectrum illustrate this for the two-spin systems Gly-25 and -44 and for the linear spin systems of Val-18 and Thr-52. It is also indicated that the $C_\alpha H$–$C_\beta H_3$ cross peaks are not completely suppressed in the TQF spectrum for Ala and Thr (e.g., Ala-50) (Muller et al., 1985). Effective suppression was, however, obtained for the methyl cross peaks of the linear Val and Leu systems and of the $C_\gamma H_3$–$C_\beta H$ moiety of Ile, which clearly exposed the Ile $C_\delta H_3$–$C_\gamma H_2$ cross peaks together with a thus far unassigned cross peak. For Ile residues 9, 48, and 65 the $C_\delta H_3$–$C_\gamma H$ cross peaks in TQF are connected with the $C_\beta H$–$C_\gamma H$ cross peaks in DQF.

S59, N64, S66, and D69 were assigned as a group from DQF spectra, where in most cases only one $C_\alpha H$–$C_\beta H$ cross peak could be observed. The other $C_\beta H$ resonance was found either from the C_β–C_β cross peak as illustrated for C54 and C55 in the DQF spectrum or, when that was impossible due to overlap of resonances, from relay spectra in which the other cross peak was observable through $C_\alpha H$–$C_\beta H$–$C_\beta H$ coherence transfer (illustrated for C55 in Figure 3). The system of S16 could not be recognized at the outset due to the (near) degeneracy of the $C_\alpha H$ and $C_\beta H$ resonances, whereas the $C_\beta H$ resonances of Cys-21 could only be obtained from NOESY connectivities in the final stages of the assignment procedure. The AMX moieties of the aromatic residues Y13, H15, Y23, F51, and H67, obtained from DQF (Figure 1) and relay (Figure 3) spectra, were connected with the ring systems of these residues by using NOE spectroscopy (not shown). Connectivities of amide protons with the aliphatic moieties of the AMX spin systems could be obtained from relay in H_2O for only eight residues; the other connectivities were found from the COSY fingerprint data (Figure 4) together with NOE data at the outset of the assignment procedure. Several AMPTX spin systems of the Met, Glu, and Gln residues could be identified as a group at the outset of the assignment procedure by using relayed spectroscopy (M0, Q3, E7, Q32, E35, Q36, M70, and Q71; Figure 3), whereas for the remaining three residues of this type the C_β resonance was identified from either relay in H_2O or DQF spectroscopy in ^2H_2O (Figures 2 and 1) and taken as originating from AMPTX spin systems on the basis of chemical shifts. Only a very small number of $NHC_\alpha HC_\beta H$ systems could be identified from relay in H_2O for the AMPTX spin systems (Figure 2). Due to overlap in the $C_\alpha HC_\beta H$ spectral region for the longer spin systems of Pro, Arg, and Lys, no initial identifications could be made at the start of the assignment procedure. The identifications given in the figures

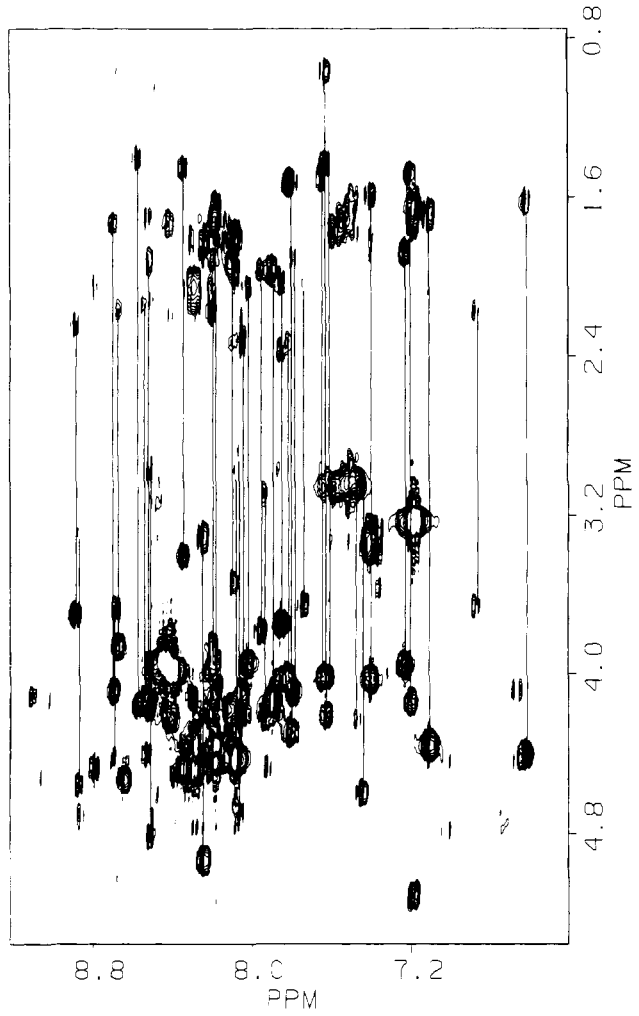

FIGURE 2: Amide proton–aliphatic protein region of a relayed coherence transfer COSY spectrum of rC5a[Met0] in 90% H_2O/10% ^2H_2O, pH 2.3, 30 °C. The spectrum was collected with the carrier at the low-field side of the spectrum. The relay evolution time was 35 ms. The H_2O resonance was suppressed by using continuous radio frequency saturation except during t_1 and t_2. The spectrum was processed by using unshifted sine bells in both dimensions in the absolute value mode. Digital resolution is 4.9 Hz/point in both dimensions. Vertical lines connect the direct cross peaks NH–C_αH and relayed cross peaks NH–C_βH for the residues (left to right) V56, N24, T33, L2, T52, V17, A10, E35, Q3, D31, A38, H15, R37, A58, I48, Y23, N64, E8, V28, V57, C47, I65, I9, Q36, A63, K4, K19, A11, A50, A26, C22, C27, K12, I41, A39, R40, V18, and L43.

were only obtained in the final stages of the sequential assignment procedure.

In summary, at the outset of the sequential assignment procedure a large number of spin systems could be identified from correlated spectroscopy. They included all of the Ala, Val, Thr, and Ile residues for which through-bond connectivities with the amide protons were obtained (except for Ile-6 and Thr-1). The large majority of the AMX and AMPTX spin systems identified could be connected to the amide proton resonances by using either COSY, NOESY or relay data. The remaining residues (one Met, one Thr, one Gly, one Ser, one Ile, three Leu, one Pro, five Arg, and eight Lys) were treated as a group together.

Sequential Assignment of the Backbone Protons. The sequential assignment of the protein was largely carried out by using spectra recorded from a protein solution in 90% H_2O/10% ^2H_2O, pH 2.35, 10 °C. These conditions were chosen for the following reasons: (i) The C5a protein is very stable at low pH; indeed, the protein is purified at those conditions. (ii) It was found to be necessary to record the spectra at conditions of nearly minimum intrinsic solvent exchange rate (pH 3.5) (Wagner, 1983b) to avoid loss of amide proton resonances in poorly structured regions of the protein (e.g., the C-terminal decapeptide). (iii) The low temperature was chosen because it allows more intense NOEs caused by a relatively slow rotational correlation time, while the position of the H_2O resonance at this temperature (4.95 ppm) allows selective presaturation without saturation of C_αH resonances except for His-15 (see Figure 5). It was found that only small chemical shift changes occurred for the side-chain resonances of the amino acids when the temperature was changed from 30 °C at which conditions the spin systems were analyzed (see above) to 10 °C, allowing those identifications to be used at the lower temperature. Larger shifts were observed for the amide proton resonance positions when the temperature was changed, only allowing positive identifications of the NH–C_αH–C_βH connectivities from relay (Figure 2) for those residues for which the NH–C_αH cross peaks are well resolved from the bulk of the fingerprint intensity. Fortunately, these resonances included most of the identified residues moieties. No additional information could be obtained from relay spectra recorded at 10 °C since the broader line width, combined with the instrinsic small value for the C_αH–NH scalar coupling constant (Pardi et al., 1984) of most of the amino acids in this protein, which turned out to be almost exclusively helical, resulted in a very poor signal to noise ratio for that experiment (results not shown).

Figure 4 shows the COSY fingerprint of rC5a[Met0] in H_2O. Out of the 77 possible NH–C_αH connectivities (rC5a[Met0] has one proline and three glycines) 53 cross peaks were sufficiently resolved to be identified, 15 occurred in crowded regions of the spectrum that did not allow a correct resonance position to be deduced, and 6 eluded observation either because of fast amide proton exchange (Met–0), saturation of the C_αH resonance (His-15), or insufficient signal to noise ratio due to a vanishingly small NH–C_αH coupling constant (S16, V18, C34, and F51). Additional very strong cross-peak intensity was observed at (ω_1, ω_2) coordinates (3.90, 8.55) and (4.68, 8.60) ppm due to the fingerprint correlations of the Gly and Cys residues in a glutathione moiety attached to Cys-27, obscuring the protein fingerprint. Further unidentified intensity occurred at coordinates (4.40, 8.70), (4.28, 8.65), (4.25, 8.42), and (4.58, 8.00) ppm, which could not be assigned at the time. Subsequent studies have shown that these cross peaks are very likely to be caused by a small fraction of random-type conformation of residues around Lys-12 (D. G. Nettesheim and E. R. P. Zuiderweg, unpublished observations).

Superior resolution in the NHC_αH spectral region was observed in the NOESY spectra of the protein (Figure 5) where the multiplet structure of the cross peaks is not exaggerated by antiphase patterns. From these spectra the exact resonance positions of the NH–C_αH correlations in the crowded regions could be inferred during the sequential resonance assignment procedure. All $d_{\alpha N}(i, i+1)$ connectivities observed in rC5a[Met0] are documented in this figure where the intraresidue NH–C_αH NOE cross peaks, coinciding with COSY fingerprint intensity, are labeled according to identity. The general procedure (Wagner & Wüthrich, 1982) for obtaining resonance assignments in this part of the spectrum, i.e., the search of NOESY cross peaks between the α proton and amide proton of residues adjacent in the sequence, denoted $d_{\alpha N}(i, i+1)$ and abbreviated as $d_{\alpha N}$, was severely complicated due to overlap of resonances and the simultaneous presence

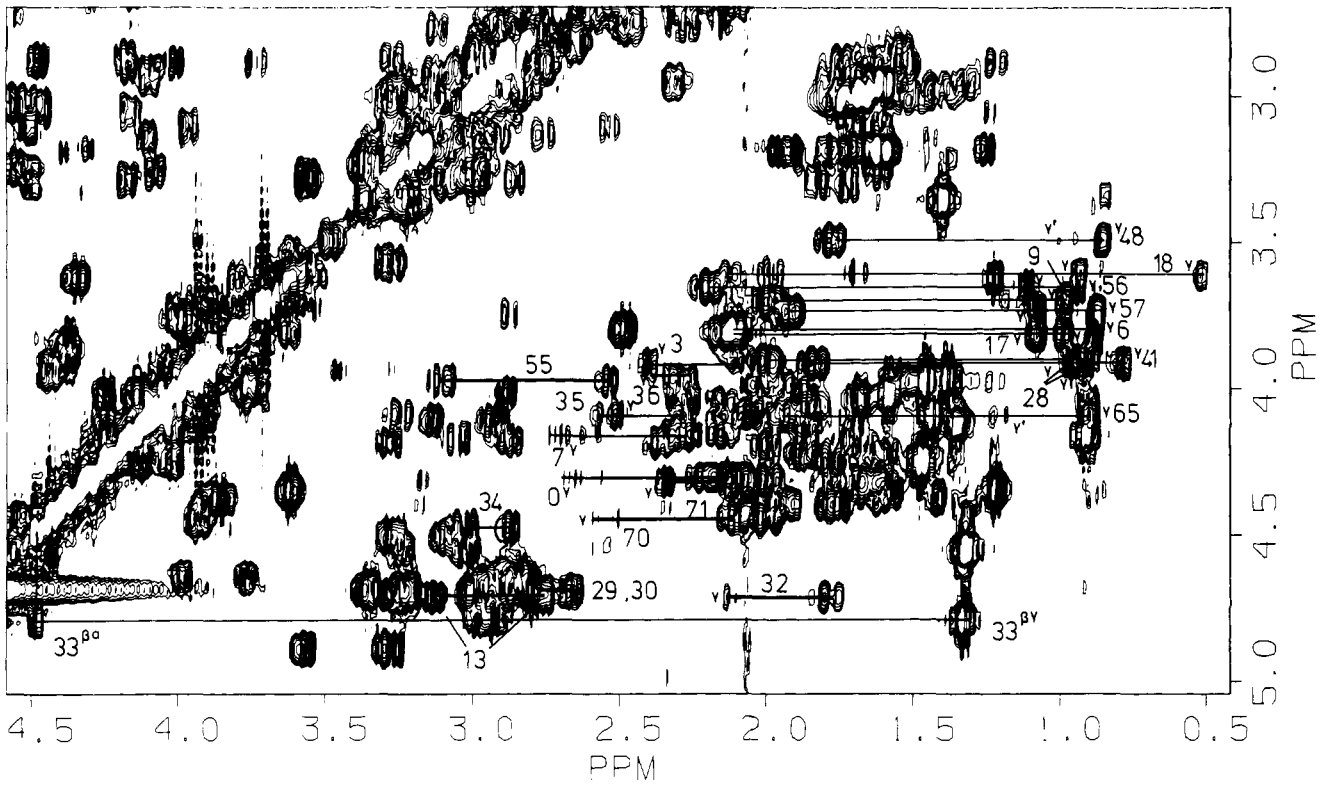

FIGURE 3: Aliphatic region of a relayed coherence transfer COSY spectrum of rC5a[Met0] in ^2H_2O, pH 2.3, 30 °C. The spectrum was collected with the carrier on the high-field side, and the relay evolution time was 35 ms. The spectrum was processed by using unshifted sine bells in both dimensions; the digital resolution is 4.9 Hz point in both dimensions and was plotted in absolute value mode. Horizontal lines connect $C_\alpha H$–$C_\beta H$ cross peaks with $C_\alpha H$–$C_\gamma H$ cross peaks indicated with γ, except for the AMX spin systems of Y13, N29, N30, C34, and C55, where the two $C_\alpha H$–$C_\beta H$ cross peaks are connected, and for Thr-33, where the entire spin system is delineated. The cross peaks labeled γ' show the relay to the γ-methylene protons for I48 and I65; for the methyl-containing residues I6, I9, V17, V18, V28, I41, I48, V56, V57, and I65 the relay to the $C_\gamma H_3$ resonances is indicated with γ.

of medium-range connectivities $d_{\alpha N}(i, i + 3)$ and $d_{\alpha N}(i, i + 4)$ in the same spectral region. Assignment of the $d_{\alpha N}$ connectivities, as documented in Figure 5, was only possible by a simultaneous analysis of the sequential amide proton resonances (d_{NN}) and $C_\beta H$–amide connectivities ($d_{\beta N}$) and by comparing spectra recorded at different experimental conditions. Conversely, delineation of d_{NN} connectivities around the amide proton diagonal (Figure 6) could be analyzed only by taking the other connectivities into account.

As an example in which several complications occurred, we follow the connectivity trajectory in the segment A58–C55 (Figure 5a, dashed lines). Starting from the intraresidue cross peak of an Alanyl residue, a $d_{\alpha N}$ cross peak with unique NH and $C_\alpha H$ coordinates (ω_2, ω_1) leads unambiguously to the $C_\alpha H$ resonance position of a valyl residue (on the horizontal axis). From there, two cross peaks are found, one leading to the $C_\alpha H$ position of an identified AMX spin system and one leading to the $C_\alpha H$ position of another Val residue. Ambiguities like these were generally resolved in one of the following ways: (i) The primary structure was checked for the occurrence of a specific sequence of amino acids (here an AMX-V-A or a V-V-A sequence). (ii) The NOE spectrum was searched for d_{NN} and $d_{\beta N}$ connectivities that would be compatible with only one of the two or more possibilities. (iii) The remaining cross peak was identified to occur from either another residue pair or from a nonsequential connectivity. For the present example all three criteria could be used: Inspection of the amino acid sequence showed that AMX-V-A does not exist in rC5a-[Met0], a strong d_{NN} connectivity was found between the amide resonances of the two Val residues (Figure 6a) as well as a $d_{\beta N}$ connectivity (spectra not shown), and the other cross peak was found to arise from a $d_{\alpha N}(i, i + 3)$ connectivity with residue 54, compatible with α-helicity in this region of the protein. Further following the trajectory A58-V57-V56 at the V56 amide proton position, five cross peaks leading to $C_\alpha H$ resonance positions are found. The strong peak leading to a $C_\alpha H$ at 4.6 ppm could be attributed to an intraresidue connectivity of another residue (D24, see Figures 4 and 5b). The unresolved cross peak just below the indicated connectivity was found to lead to a long side chain residue (Lys-20) and could thus be excluded by inspecting the amino acid sequence in which no long side chain Cys-Val-Val-Ala sequence exists. All three other peaks, however, led to AMX spin systems, as a consequence of which no decision could be made since a Cys residue is expected at the N terminus of the peptide segment under consideration. Obviously, the search for d_{NN} and $d_{\beta N}$ connectivities does not resolve the ambiguities since the amide proton resonances of D24 and Val-56 are degenerate. In cases like this, we reverted to the inspection of spectra recorded at different experimental conditions in which the chance degeneracy of the amide protons of Val-56 and Asp-24 did not occur (data not shown) and to spectra of rC5a[Met0] recorded from a rC5a[Met0] solution in ^2H_2O where the amide proton of Asp-24 was exchanged for a deuteron while the amide proton of Val-56, including its NOE connectivities, was still present (data will be published in a forthcoming paper). Thus, the cross peak as indicated in Figure 6a was identified to lead to the $C_\alpha H$ position of Cys-55. Its amide position could subsequently be inferred from the d_{NN} (Figure 6a) and $d_{\beta N}$ connectivities. Thus, although no well-defined NH-$C_\alpha H$ cross peak could be found in the COSY fingerprint for this residue (Figure 4), its coordinates could be derived with accuracy from the NOE data as described. Parenthetically, the other cross peaks at the amide proton position of Val-56 could be identified

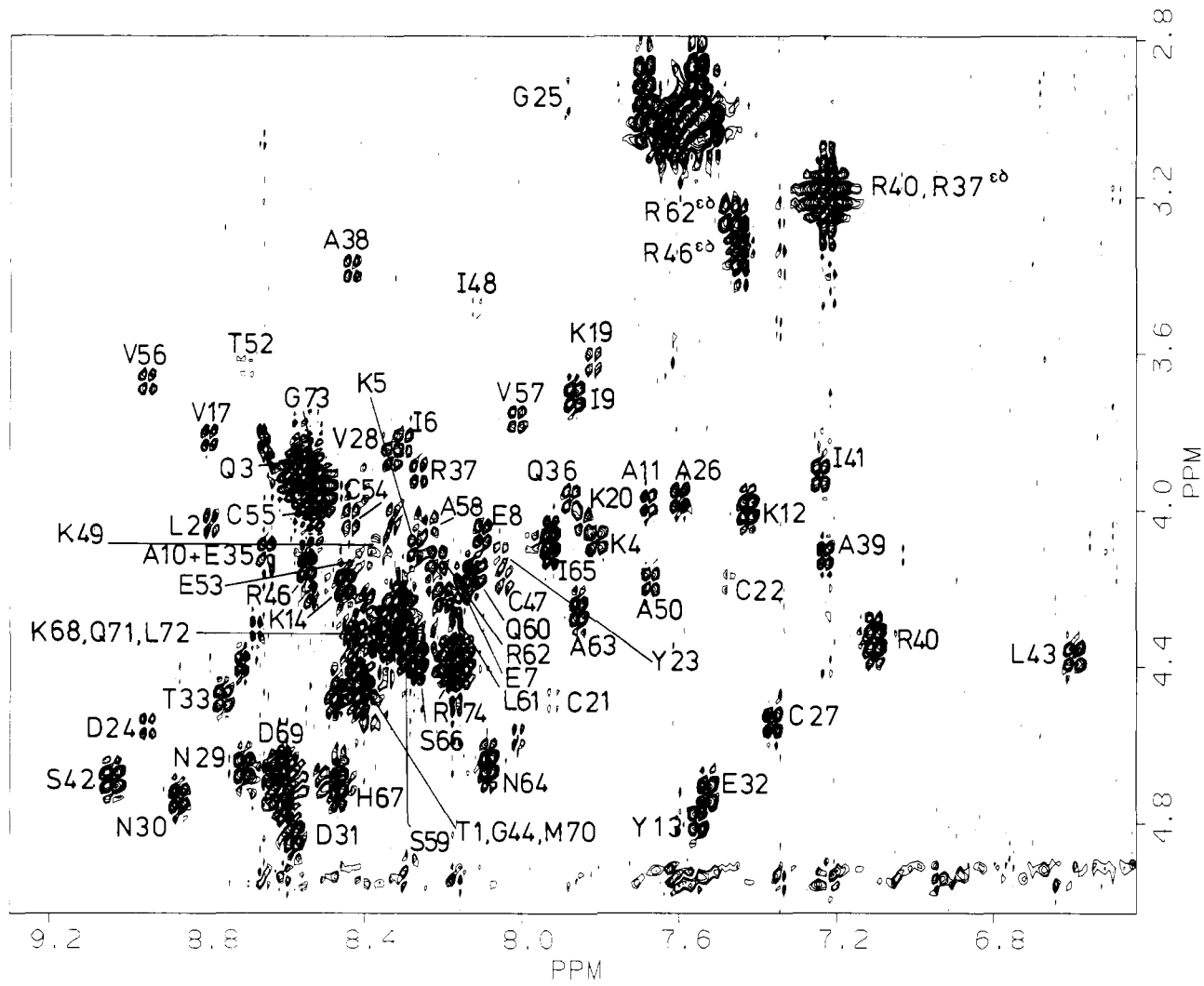

FIGURE 4: Fingerprint region of the phase-sensitive COSY spectrum of rC5a[met0] in 90% H_2O/10% ^2H_2O, pH 2.3, 10 °C. The solvent resonance was suppressed by continuous radio frequency saturation at all times except during t_1 and t_2. The data were processed with unshifted sine-bell functions in both dimensions; the digital resolution is 4.9 Hz/point in both dimensions. Positive and negative contour levels are shown. NH–C_αH cross peaks are identified by the labels. The cross peaks for the arginyl residues at the upper right hand region of the spectrum are N_ϵH–C_δH connectivities for these residues. The large unassigned patch of intensity at (7.6, 3.0) ppm arises from the Lys side chains.

as $d_{\alpha N}(i, i + 3)$, $d_{\alpha N}(i, i + 1)$, and $d_{\alpha N}(i, i + 4)$ for the residue pairs C21–D24, Y23–D24, and K20–D24 from low to high field in ω_1, respectively. Along similar lines of argumentation, all cross peaks in the fingerprint part of the NOESY spectrum could be assigned to intraresidue, $d_{\alpha N}(i, i + 1)$, $d_{\alpha N}(i, i + 3)$, or $d_{\alpha N}(i, i + 4)$ connectivities. The latter distance is 4.1 Å in regular helical structure. Only a few long-range NOEs could be observed in this region of the spectrum.

As an example of the tracing of connectivities between adjacent amide protons (d_{NN}), we describe the stretch 46–53 (Figure 6a). Starting at the nondegenerate amide proton of a threonyl residue, assigned as such prior to sequential assignment (see Figure 2), we find a cross peak (labeled 52/51) connecting to the nondegenerate amide resonance of a residue for which no COSY fingerprint cross peak could be found. From there, a strong cross peak leads to the resolved NH resonance of a residue identified as Ala prior to sequential assignment. Inspection of the primary structure for a sequence Thr-X-Ala or Ala-X-Thr shows that only one such stretch occurs in rC5a[Met0] (T52-F51-A50), allowing the assignment of these amide protons as well as the assignment of the C_αH and side-chain protons of Phe-51. Once this tripeptide was identified, the well-resolved cross peak to Glu-53 could be identified (labeled 53/52) as well as the peak leading to Lys-49 (labeled 50/49). In the search for a d_{NN} connectivity between Lys-49 and Ile-48 only one intensity (labeled 48/49) coincided with the amide proton position of an identified Ile residue. This assignment could be verified from a well-resolved weak $d_{\alpha N}$ connectivity between these residues (Figure 5b). Intensity close to the diagonal (labeled 47/48) coincided with the amide proton position of a AMX spin system that was assigned to Cys-47 after verification obtained from a $d_{\beta N}$ connectivity between these residues (not shown). From the amide proton position of Cys-47 a strong cross peak was observed to an amide proton of a thusfar unidentified (long side chain) residue with an unique chemical shift. This residue was thus identified as Arg-46, after verification of the existence of a $d_{\beta N}$ connectivity between these residues (not shown) and by recognizing the well-defined termination of the d_{NN} stretch at this residue, which is to be expected since its neighboring residue is a proline. Analogous arguments were used to identify the remaining d_{NN} connectivities in the spectrum of rC5a[Met0] (Figure 6). As a result, all of the cross peaks in this region of the spectrum were assigned to either specific adjacent residue pairs, to NOEs between amide protons and aromatic residues (predominantly Phe-51), or to NOEs between ring protons of aromatic residues and between the peripheral exchangeable protons of Asn and Gln residues (Figure 6c). In two cases evidence was found for $d_{NN}(i, i + 2)$ connectivities in this region of the spectrum (between C47 and

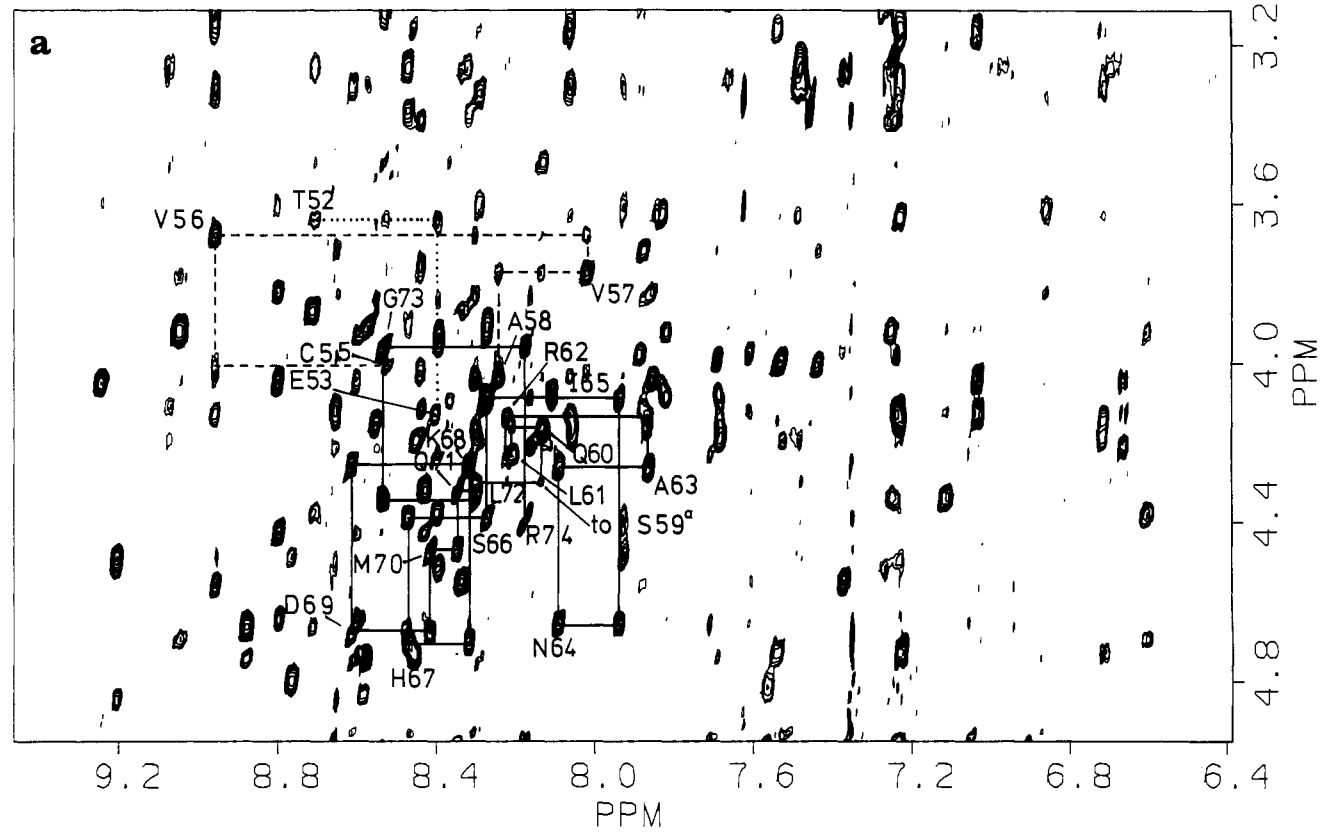
a
V56
T52
V57
G73
A58
C55
R62
E53
I65
K68
Q71
Q60
A63
L72
L61
to
S59α
S66
R74
M70
D69
N64
H67
9.2
8.8
8.4
8.0
7.6
7.2
6.8
6.4
PPM
3.2
3.6
4.0
4.4
4.8
PPM

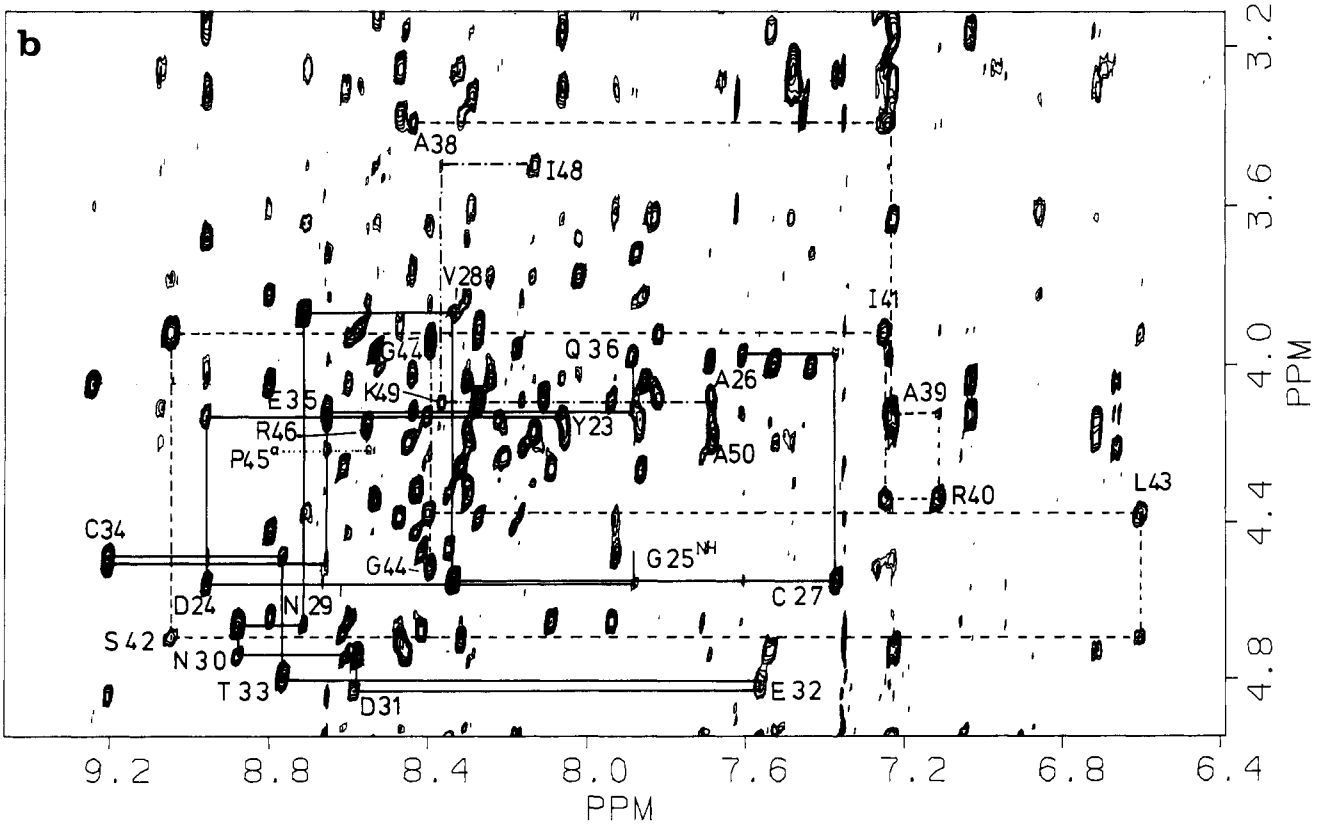
b
A38
I48
V28
I41
G44
Q36
A26
A39
E35
K49
Y23
R46
P45α
A50
R40
L43
C34
G44
G25NH
C27
D24
N29
S42
N30
T33
E32
D31
9.2
8.8
8.4
8.0
7.6
7.2
6.8
6.4
PPM
3.2
3.6
4.0
4.4
4.8
PPM

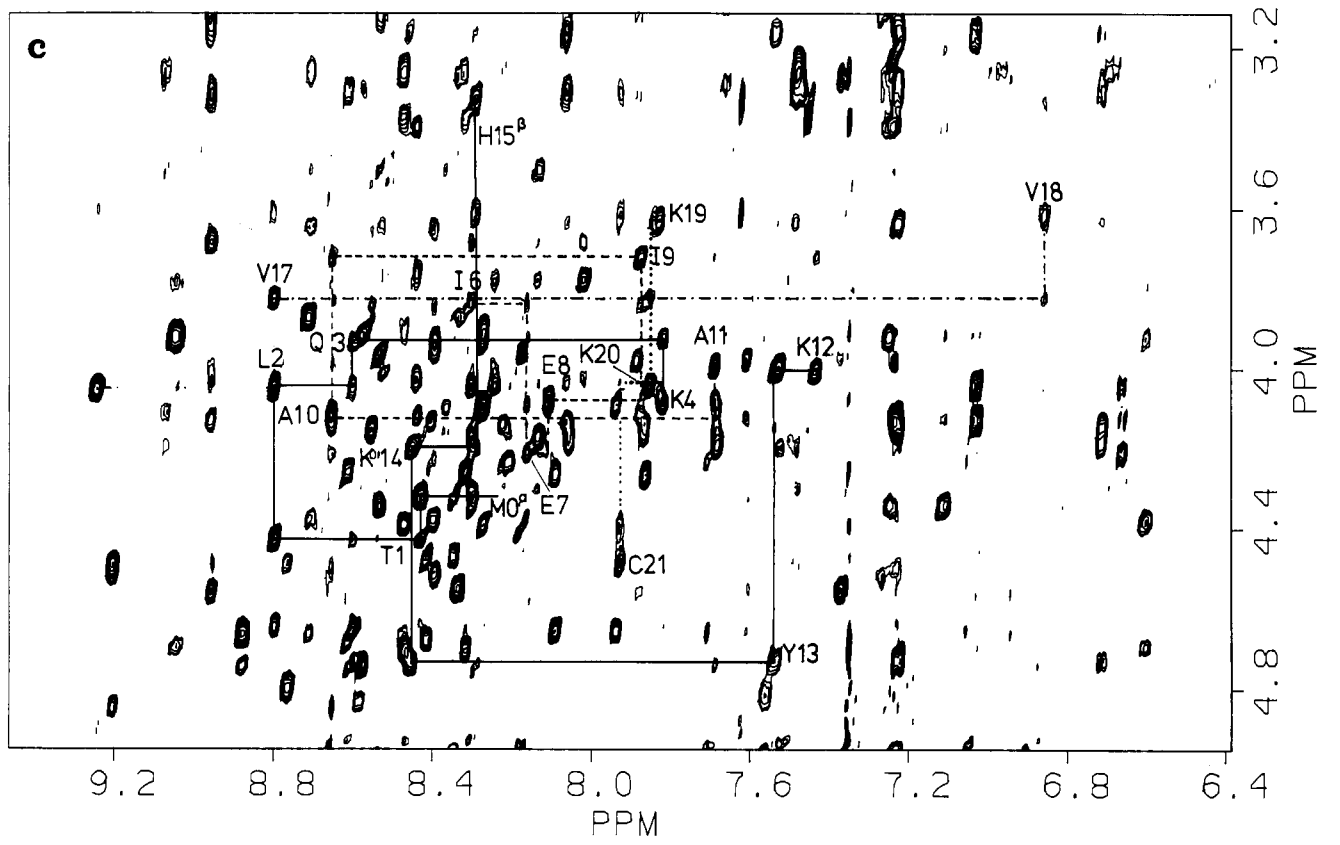

FIGURE 5: Fingerprint region of a phase-sensitive NOESY spectrum or rC5a[Met0] in 90% H_2O/10% ^2H_2O, pH 2.3, 10 °C. The solvent resonance was suppressed by continuous observe field coherent time-shared radio frequency saturation at all times except during t_1 and t_2. The NOE mixing time was 100 ms. The spectrum was processed by using an unshifted sine bell in t_2 and a sine bell shifted by 30° in t_1. The digital resolution is 2.5 Hz/point in ω_2 and 4.9 Hz/point in ω_1. In this figure all observed $d_{\alpha N}$ cross peaks observed are documented; they are found at the intersections of the horizontal and vertical lines leading to the intraresidue NOEs identified by labels. (a) Connectivities in the regions 52–53 (···), 55–58 (- - -), and 59–74 (—). (b) Connectivities in the regions 23–25 (—), 26–36 (—), 38–44 (- - -), and 48–50 (-·-). (c) Connectivities in the regions 0–4 (—), 7–11 (- - -), 12–15 (—), 17–18 (-·-), and 19–21 (···).

K49 and between V17 and K19, Figure 6a,b). The distance between such protons is 4.2 Å in helical secondary structure.

The obtained connectivities are shown in Figure 7, in which it can be seen that at least one of the NH, $C_\alpha H$, or $C_\beta H$ protons for all residues was assigned by using sequential connectivities. The overlap of sequential connectivities is interrupted between Lys-5 and Ile-6, where the $d_{\alpha N}$ cross peak is missing, the $d_{\beta N}$ cross peak was not observed because of overlap, and the d_{NN}, if present, was too close to the amide proton diagonal to allow detection. The observation of a well-resolved medium-range NOE $d_{\alpha N}(i, i + 3)$ between Lys-4 and Glu-7 provided, however, a connection of the assignments of the first six residues with those of the remainder of the protein (results shown in a forthcoming paper). Well-defined cross peaks between one of the α protons of Gly-44 and a pair of resonances at 3.64 and 3.86 ppm were observed in the NOE spectrum of rC5a[Met0] in ^2H_2O (results shown in a forthcoming paper). Since these latter resonances were the only unassigned coupled resonances in this part of a TQF spectrum (Figure 1) after the full assignment of all AMX spin systems, they could be confidently assigned to the δ protons of Pro-45. Thus, the NOE cross peaks between G44 and P45 provided the continuity in assignments in this part of the protein. Independent checks on the assignments were made from spectra of rC5a[Met0] in which parts of the amide protons were exchanged for deuterons. The assignment patterns could be followed in contiguous segments of resolved slowly exchanging protons. Furthermore, a rC5a[Met0] derivative, in which the last 11 amino acids were removed by enzymatic cleavage, was studied by NMR. All assignments of the first 60 residues could be traced in this molecule where only small chemical shift changes were observed except at the C terminus (D. G. Nettesheim and E. R. P. Zuiderweg, unpublished results). Finally, a large amount of medium-range NOE connectivities $d_{\alpha N}(i, i + 3)$, $d_{\alpha N}(i, i + 4)$, and $d_{\alpha\beta}(i, i + 3)$ could be traced in the NOE spectra, further adding confidence in the described assignments.

Additional Assignments. Once the sequence-specific assignments were obtained for all of the backbone protons of rC5a[Met0], it was possible to obtain additional assignments for protons in the amino acid side chains. Thus, assignments could be found for the majority of the β protons of the Arg and Lys side chains by identifying the proper DQF COSY $C_\alpha H$–$C_\beta H$ cross peaks (Figure 2) at positions as inferred from the NH–$C_\beta H$ intra- and interresidue NOEs in the spectrum of rC5a[Met0] in H_2O. Well-defined NOE cross peaks were observed between the β protons of Asn residues and γ protons of Gln residues and peripheral amide protons. These cross peaks, in conjunction with very strong NOE cross peaks between pairs of peripheral amide protons, were used to assign the $N_\delta H_2$ and $N_\epsilon H_2$ protons of all of the Asn and Gln residues except Gln-60. The remaining peripheral amide proton cross peaks could thus be assigned to Gln-60 by exclusion. These assignments are shown in Figure 6c. A subset of the ring protons of the aromatic residues was assigned by using NOEs from the assigned $C_\alpha H$ resonances to the C2, 6H, or C4H ring protons of the Tyr, Phe, and His residues, respectively. The assignments for the other ring proton resonances were easily obtained from a 2D double-quantum spectrum for the Tyr and His residues (see Figure 8). A well-resolved connectivity was found in this spectrum between the F51 ring protons. Integration of the resonances in the 1D spectrum showed that this

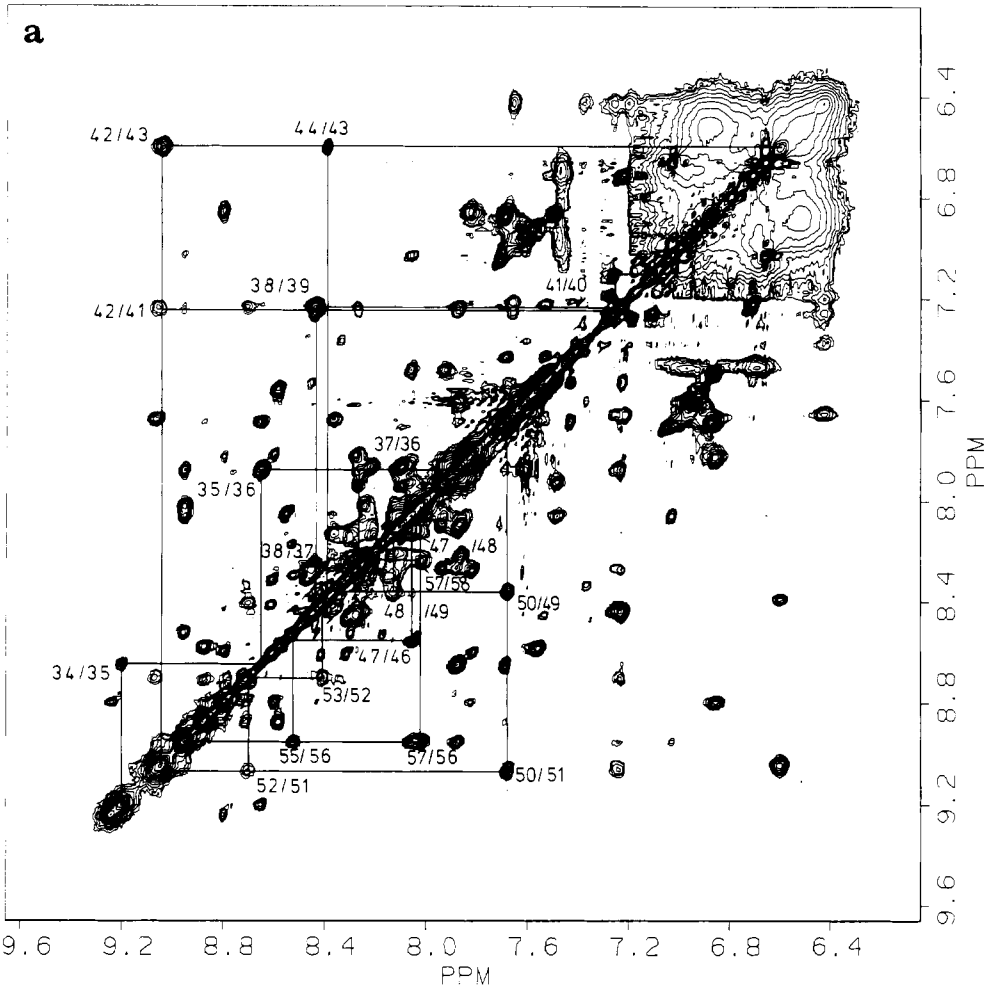
a
42/43
44/43
38/39
41/40
42/41
37/36
35/36
38/37
47/48
57/58
50/49
48/49
47/46
34/35
53/52
55/56
57/56
50/51
52/51
9.6 9.2 8.8 8.4 8.0 7.6 7.2 6.8 6.4
PPM

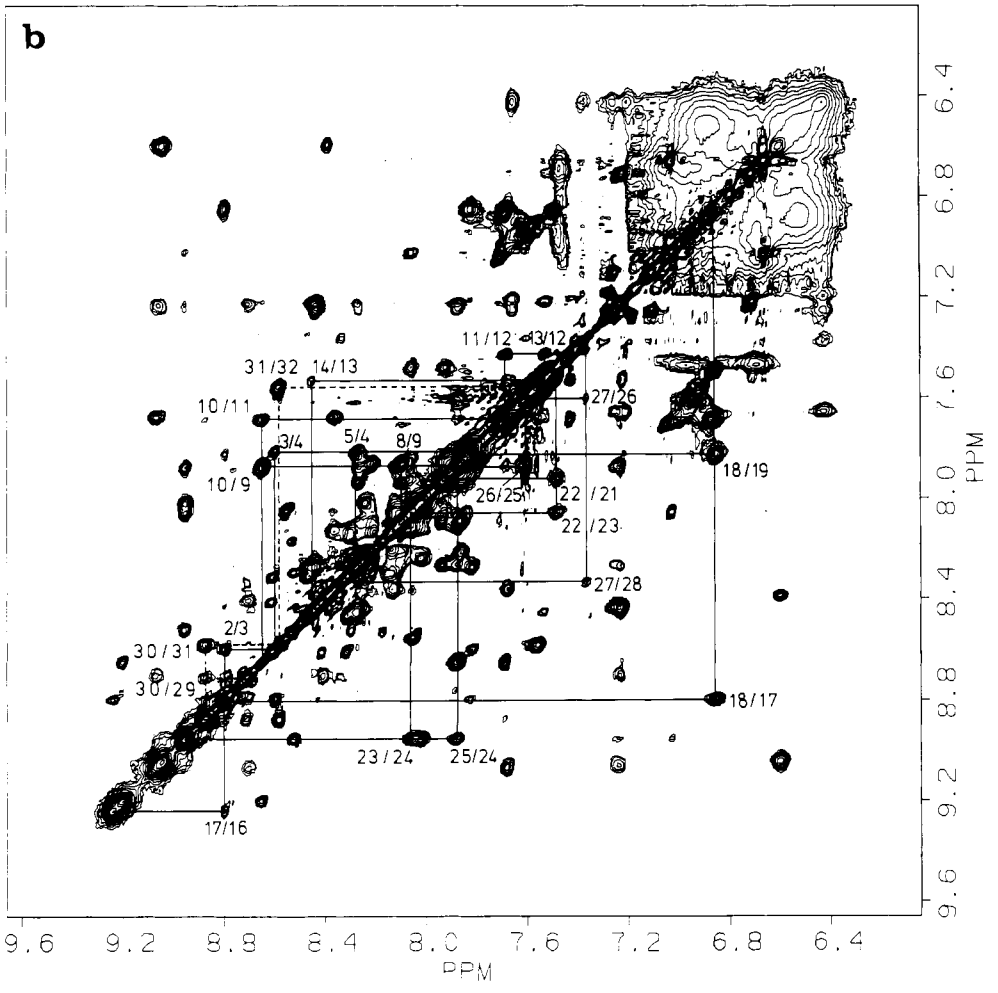
b
11/12
13/12
31/32
14/13
27/26
10/11
5/4
8/9
18/19
10/9
26/25
22/21
22/23
27/28
2/3
30/31
30/29
18/17
23/24
25/24
17/16
9.6 9.2 8.8 8.4 8.0 7.6 7.2 6.8 6.4
PPM

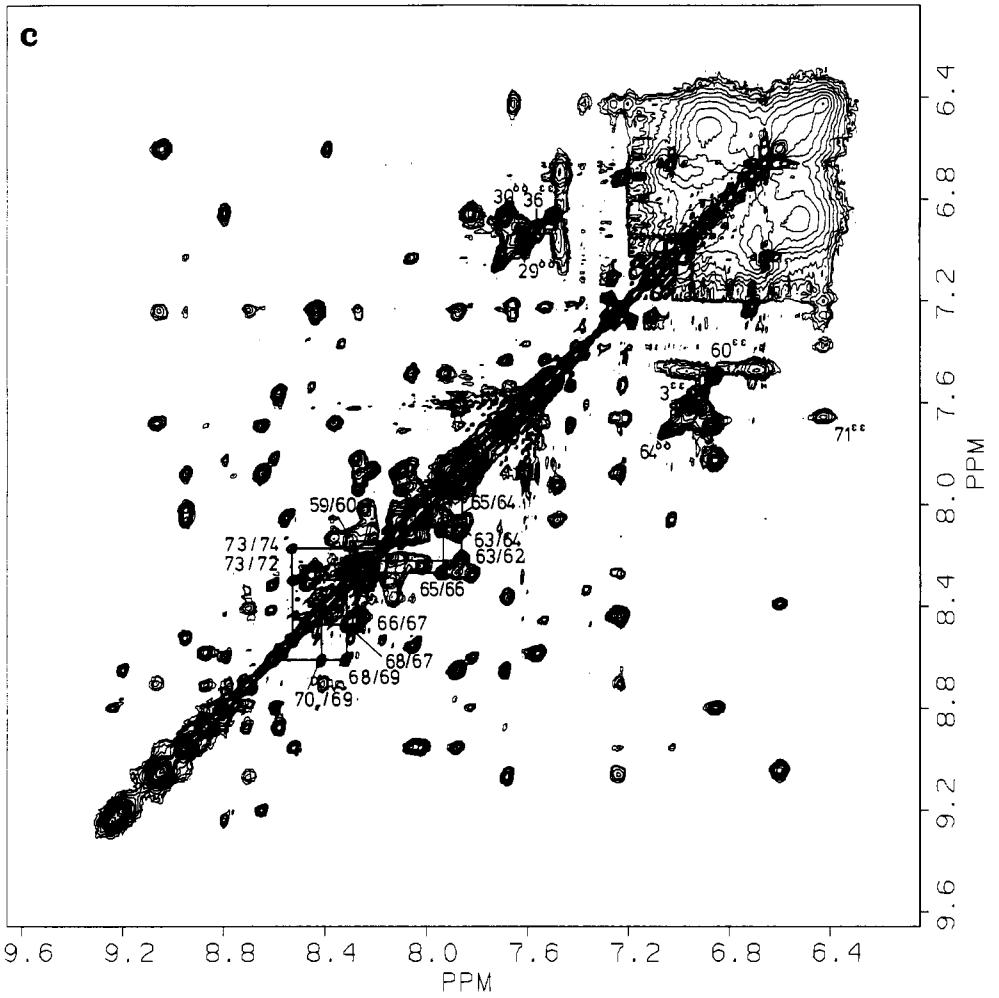

FIGURE 6: d_{NN} region of a phase-sensitive NOESY spectrum or rC5a[Met0] in 90% H_2O/10% ^2H_2O, pH 2.3, 10 °C. The solvent resonance was suppressed by continuous observe field coherent time-shared radio frequency saturation at all times except during t_1 and t_2. The NOE mixing time was 100 ms. The spectrum was processed by using a sine bell shifted by 30° in both dimensions, and the digital resolution was 4.9 Hz/point in both dimensions. The data are symmetrized. In this figure all observed d_{NN} cross peaks observed are documented. The cross peaks are labeled NH(ω_2)/NH(ω_1); vertical and horizontal lines lead to the diagonal positions of the amide protons. (a) Connectivities in the regions 34–39 (top triangle), 40–44 (top triangle), 46–53 (bottom triangle), and 55–58 (bottom triangle). (b) Connectivities in the regions 2–5 (top triangle), 8–14 (top triangle), 16–19 (bottom triangle), 21–28 (bottom triangle), and 29–32 (top triangle; dashed). (c) Connectivities in the regions 59–60 (top triangle), 62–70 (bottom triangle), and 72–74 (top triangle). Also indicated in (c) are the $N_\delta H$–$N_\delta H$ NOE connectivities for the Asn residues and the $N_\epsilon H$–$N_\epsilon H$ NOE connectivities for the Gln residues.

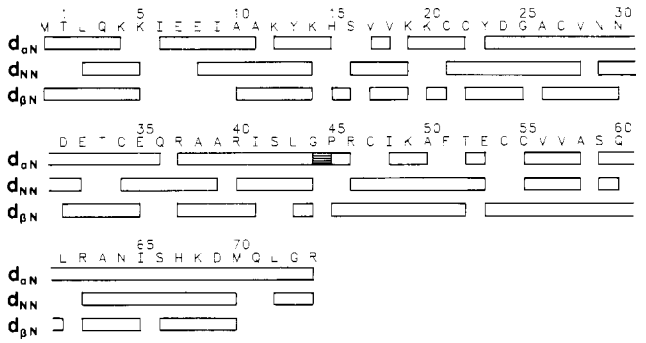

FIGURE 7: Overview of the obtained sequential connectivities for the NMR spectrum of rC5a[Met0] at pH 2.3, 10 °C. Boxes indicate the observed connectivities; the hatched box between Gly-44 and Pro-45 represents the $d_{\alpha\delta}$ connectivity observed between those residues.

connectivity leads to a multiplet of unit proton intensity, which was therefore assigned to originate from the Phe-51 C4 proton (see Figure 8). Additional peripheral resonances were assigned for the arginyl residues by utilizing the $N_\epsilon H$ resonances for these residues as identified from arginyl $N_\epsilon H$–$C_\delta H_2$ correlations found in the COSY fingerprint region. Three of these exchangeable proton lines showed NOEs to the β protons of the assigned Arg residues (40, 46, and 62), thereby allowing sequence-specific assignments of the $N_\epsilon H$ and $C_\delta H$ protons (via COSY) of these residues. NOE cross peaks were found leading from the $C_\alpha H$ and $C_\beta H$ resonances of Arg-37 to a pair of C_δ protons, at a resonance position corresponding to the coordinates of a $N_\epsilon H$–$C_\delta H$ cross peak in the COSY fingerprint. Consequently, this cross peak was used for the assignment of these resonances of Arg-37. These assignments are indicated in the fingerprint region of the COSY spectrum (Figure 4). No through-bond connectivities were observed to allow the connection of the methyl groups of the three leucine residues to the $NHC_\alpha HC_\beta H$ moieties of these residues. Therefore, the methyl groups for these residues were identified from the (spin diffusive) intraresidue NOEs between the amide proton and these groups, combined with sequential-type NOEs of the amide protons of adjacent residues with these methyl groups for the Leu residues 2 and 61.

Discussion

In Table I all assignments obtained for the ^1H NMR spectrum of rC5a[Met0] at pH 2.3, 10 °C, are listed. The table shows that all the backbone proton resonances for all residues have been assigned, that full side-chain proton assignments were obtained for 57 residues, and that the unassigned protons belong exclusively to Lys, Arg, Pro, and Leu

Table I: ^{1}H Resonance Assignments for rC5a[Met0], pH 2.3, 10 °C[a]

residue	NH	αCH	βCH	γCH	others
Met-0		4.33	2.25	2.58, 2.70	SCH_3 2.09[b]
Thr-1	8.42	4.43	4.64	1.38	
Leu-2	8.79	4.04	1.70, 1.75	1.78[c]	δCH_3 0.95,[c] 1.01[c]
Gln-3	8.60	3.93	2.00, 2.14	2.45	ϵNH_2 6.92, 7.57
Lys-4	7.82	4.10	1.90		
Lys-5	8.28	4.11			
Ile-6	8.30	3.84	2.20	1.42, 1.73	γCH_3 0.92, δCH_3 0.79
Glu-7	8.17	4.23	2.24, 2.36	2.68, 2.78	
Glu-8	8.11	4.09	2.20, 2.32	2.50, 2.81	
Ile-9	7.88	3.74	2.05	1.21, 1.87	γCH_3 1.05, δCH_3 0.94
Ala-10	8.65	4.13	1.37		
Ala-11	7.70	4.01	1.51		
Lys-12	7.44	4.02	1.60		
Tyr-13	7.54	4.74	2.82, 3.17		C2,6H 7.24, C3,5H 6.73
Lys-14	8.45	4.22	1.74		
His-15	8.29	4.92	3.36, 3.63		C2H 8.76, C4H 7.63
Ser-16	9.24	4.07	4.07		
Val-17	8.80	3.84	2.16	1.07, 1.15	
Val-18	6.87	3.63	2.21	0.58, 1.00	
Lys-19	7.84	3.64	2.03		
Lys-20	7.86	4.06			
Cys-21	7.93	4.51	3.33,[c] 4.41[c]		
Cys-22	7.49	4.20	2.90, 3.33		
Tyr-23	8.06	4.14	2.95, 3.17		C2,6H 7.04, C3,5H 6.68
Asp-24	8.96	4.57	3.12, 3.33		
Gly-25	7.89	2.34, 2.97			
Ala-26	7.62	3.98	1.44		
Cys-27	7.38	4.56	3.05, 3.28		
Val-28	8.34	3.88	2.02	0.96, 1.03	
Asn-29	8.71	4.67	2.68, 2.86		δNH_2 6.96, 7.63
Asn-30	8.88	4.75	2.74, 2.97		δNH_2 6.89, 7.69
Asp-31	8.58	4.84	2.98		
Glu-32	7.56	4.81	2.44	1.75	
Thr-33	8.76	4.50	4.86	1.38	
Cys-34	9.20	4.51	2.92, 3.08		
Glu-35	8.66	4.13	2.05, 2.15	2.59	
Gln-36	7.88	3.98	2.35	2.49	ϵNH_2 6.96, 7.62
Arg-37	8.28	3.92	2.08, 2.40		δCH_2 3.31,[c] ϵNH 7.24[c]
Ala-38	8.44	3.41	1.48		
Ala-39	7.24	4.14	1.49		
Arg-40	7.12	4.35	2.08		δCH_2 3.21, ϵNH 7.24
Ile-41	7.26	3.94	1.90	0.90, 1.13	γCH_3 0.86, δCH_3 0.25
Ser-42	9.05	4.71	3.80, 4.05		
Leu-43	6.60	4.38	1.70		δCH_3 0.89,[c] 0.97[c]
Gly-44	8.39	3.95, 4.52			
Pro-45		4.23	2.26, 2.38		δCH_2 3.64, 3.86
Arg-46	8.55	4.17	1.90		δCH_2 3.38, ϵNH 7.47
Cys-47	8.05	4.19	3.08		
Ile-48	8.13	3.52	1.80	1.03, 1.56	γCH_3 0.88, δCH_3 0.78
Lys-49	8.37	4.12	2.00		
Ala-50	7.68	4.21	0.94		
Phe-51	9.07	4.13	2.95, 3.28		C2,3,5,6H 7.28, C4H 7.22
Thr-52	8.70	3.66	4.38	1.28	
Glu-53	8.40	4.15	2.20, 2.33	2.54	
Cys-54	8.43	4.04	2.92, 3.78		
Cys-55	8.53	4.03	2.57, 3.13		
Val-56	8.96	3.69	2.24	1.00, 1.17	
Val-57	8.02	3.79	1.96	0.94, 1.14	
Ala-58	8.25	4.05	1.65		
Ser-59	8.30	4.28	4.03, 4.17		
Gln-60	8.14	4.18	2.44	2.45,[c] 2.63[c]	ϵNH_2 6.88,[c] 7.52[c]
Leu-61	8.21	4.24	1.45	1.63[c]	δCH_3 0.95[c]
Arg-62	8.23	4.16	1.92		δCH_2 3.27, ϵNH 7.49
Ala-63	7.87	4.28	1.55		
Asn-64	8.09	4.67	2.90, 2.95		δNH_2 7.06, 7.72
Ile-65	7.94	4.10	1.97	1.27, 1.64	γCH_3 0.96, δCH_3 0.96
Ser-66	8.27	4.39	3.91, 3.95		
His-67	8.47	4.72	3.27, 3.38		C2H 8.67, C4H 7.36
Lys-68	8.32	4.27	1.85		
Asp-69	8.61	4.68	2.92, 3.03		
Met-70	8.41	4.48	2.05, 2.16	2.56, 2.65	SCH_3 2.09[b]
Gln-71	8.35	4.34	2.11	2.40	ϵNH_2 7.67, 6.42
Leu-72	8.30	4.36			δCH_3 1.00[c]
Gly-73	8.53	3.98			
Arg-74	8.18	4.42	1.80		

[a] Chemical shifts with respect to 3-(trimethylsilyl)propionic acid are accurate within 0.01 ppm. [b] Chemical shift was obtained from the comparison of spectra of rC5a and rC5a [Met0]. [c] Chemical shifts, compatible with all available data, were obtained from NOESY data only.

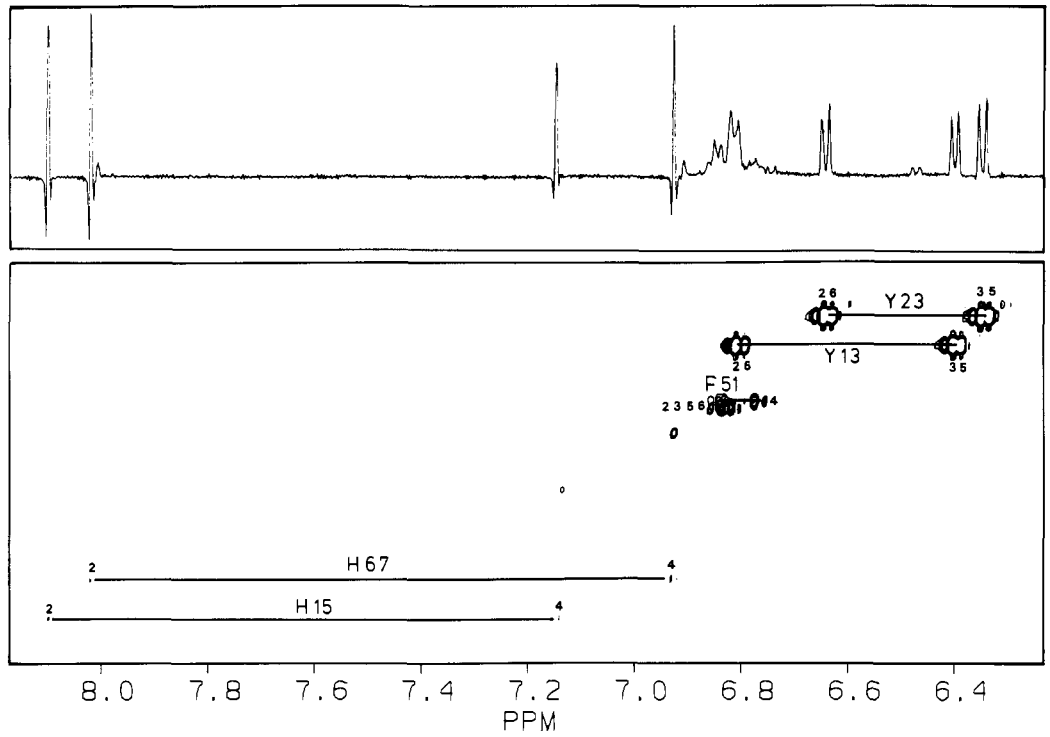

FIGURE 8: Aromatic region of a 2D double-quantum spectrum of rC5a[Met0] in ^2H_2O, pH 2.3, 10 °C. The spectrum was processed by using an unshifted sine bell in both dimensions; the digital resolution is 2.5 Hz/point in ω_2 and 10 Hz/point in ω_1. The horizontal lines connect the ring proton resonance positions as labeled. For purposes of comparison, a resolution-enhanced 1D spectrum of rC5a[Met0] is plotted at the top of the figure. Additional Tyr ring proton resonances due to the aging of the sample are observed at 6.5 and 6.75 ppm.

residues. Attempts to identify the latter protons using total correlation/homonuclear Hartmann–Hahn spectroscopy (Braunschweiler & Ernst, 1983; Bax & Davis, 1985) and double relayed COSY (Wagner, 1983a) spectra have not been successful thus far due to signal to noise ratio limitations. The obtained assignments provide an extensive data basis for the interpretation of the remaining connectivities in NOESY spectra for purposes of structural determination of the protein (Zuiderweg et al., 1988; Zuiderweg, forthcoming publication).

The results were obtained by using a combination of different types of scalar correlated spectroscopy for spin-system analysis in which especially the comparison of DQF and TQF spectra proved useful by the editing of two-spin and linear spin systems. Extensive use was made of relayed spectroscopy, not only to obtain correlations between protons separated by more than three chemical bonds but also to obtain correlations between protons that have a vanishingly small J-coupling due to conformational reasons (e.g., C_α–C_βH correlation through C_αH–$C_{\beta'}$H–C_βH relay). The sequential assignments were derived by using the classical NOE connectivities $d_{\alpha N}$, d_{NN}, and $d_{\beta N}$. Additional information, such as $d_{\alpha N}(i, i + 3)$ and $d_{\alpha N}(i, i + 4)$ connectivities, once the secondary structure became apparent, was, however, extensively used to verify the results and was also used to provide clues to the solution of the assignment puzzle. Furthermore, comparison of stretches of slowly exchanging amide protons as well as comparison with spectra recorded at different experimental conditions were indispensable tools for the disentanglement of overlapping cross peaks in the 2D spectra. It appears that if computer algorithms for the assignment of protein spectra become available, that such algorithms should be made capable of dealing with cross-peak overlap such as described in this paper in order to be useful. One possibility may be to allow an input of multiple data sets that were recorded at (slightly) different experimental conditions from which partial assignments are obtained by such an algorithm. These partial assignments could then be joined to obtain a full assignment at a particular condition.

It is of interest to ask what can be learned about the (secondary) structure of a protein from the mere knowledge of the chemical shift dispersion of resonances, especially from the amide and low-field-shifted α protons, which are readily accessible in 1D studies of small quantities of sample. In rC5a[Met0], virtually no C_α protons resonate low field of the H_2O signal at normal temperature conditions, while the bulk of the amide protons resonate in a relatively small frequency region centered around 8.2 ppm. rC5a[Met0] was found to be a protein of high α-helical content as follows from the large number of contiguous stretches of amide–amide proton NOE connectivities observed. Exact delineation of these helical stretches will be described in a following publication; they are found in the regions 3–12, 17–26, 34–39, and 45–63. For other predominantly α-helical proteins, a similar limited dispersion of the chemical shifts of amide and C_α protons was observed in contrast to proteins [e.g., BPTI (Wagner & Wüthrich, 1982), BUSI II (Strop et al., 1983), and Tendamistat (Kline & Wüthrich, 1986)] in which a large amount of extended secondary structure is present (Wagner et al., 1983). Indeed, a correlation seems to emerge that low-field-shifted C_αH resonances (>4.8 ppm) occurring in α-helical proteins occur in extended parts of these proteins [e.g., H15, S16, N30, N31, Q32, and S42 in C5a[Met0]; S2, C3, C4, C32, I35, and N45 in Phoratoxin (Clore et al., 1987); T5 and V15 in *lac*-repressor headpiece (Zuiderweg et al., 1983)]. These observations may provide clues to the assignment of α-helical proteins in the future and at the same time indicate that a size limitation for the feasibility of a full resonance assignment using ^1H NMR only might be reached somewhat earlier for α-helical proteins, in which limited chemical shift dispersion occurs, than for β-structured proteins.

ACKNOWLEDGMENTS

We thank M. Seavy, L. Fayer, and R. Edalji for their

contribution to the purification efforts of the different C5a species. We also thank Dr. S. Spanton for the maintenance of the NMR spectrometer and for writing the software for data transfer to the VAX computer.

Registry No. C5a, 80295-54-1.

REFERENCES

Aue, W. P., Bartholdi, E., & Ernst, R. R. (1976) *J. Chem. Phys. 64*, 2229.
Bax, A., & Davis, D. G. (1985) *J. Magn. Reson. 65*, 355.
Billeter, M., Braun, W., & Wüthrich, K. (1982) *J. Mol. Biol. 155*, 321.
Braun, W., Wider, G., Lee, K. H., & Wüthrich, K. (1983) *J. Mol. Biol. 169*, 921.
Braunschweiler, L., & Ernst, R. R. (1983) *J. Magn. Reson. 53*, 521.
Braunschweiler, L., Bodenhausen, G., & Ernst, R. R. (1983) *Mol. Phys. 48*, 535.
Carter, G. W., Mollison, K. W., Fayer, L., Fey, T., Krause, R., Henkin, J., & Edalji, R. (1986) *Complement 2*, 15.
Clore, G. M., Sukumaran, D. K., Nilges, M., & Gronenborn, A. M. (1987) *Biochemistry 26*, 1732.
Cooke, R. M., Wilkinson, A. J., Baron, M., Pastore, A., Tappin, M. J., Campbell, I. D., Gregory, H., & Sheard, B. (1987) *Nature (London) 327*, 339.
Fernandez, H. N., & Hugli, T. E. (1978) *J. Biol. Chem. 253*, 6955.
Greer, J. (1985) *Science (Washington, D.C.) 228*, 1055.
Huber, R., Scholze, H., Paques, E. P., & Deisenhofer, J. (1980) *Hoppe-Seyler's Z. Physiol. Chem. 361*, 1389.
Hugli, T. E. (1981) *Crit. Rev. Immunol. 1*, 321.
Jeener, J., Meier, B. H., Bachmann, P., & Ernst, R. R. (1979) *J. Chem. Phys. 71*, 4546.
Klevit, R. E., & Waygood, E. B. (1986) *Biochemistry 25*, 7774.
Kline, A. D., & Wüthrich, K. (1986) *J. Mol. Biol. 192*, 869.
Kline, A. D., Braun, W., & Wüthrich, K. (1986) *J. Mol. Biol. 189*, 377.
Mandecki, W., Mollison, K. W., Bolling, T. J., Powell, B. S., Carter, G. W., & Fox, J. L. (1985) *Proc. Natl. Acad. Sci. U.S.A. 82*, 3543.
Mandecki, W., Powell, B. S., Mollison, K. W., Carter, G. W., & Fox, J. L. (1986) *Gene 43*, 131.
Marion, D., & Wüthrich, K. (1983) *Biochem. Biophys. Res. Commun. 113*, 967.
Mayer, M. M. (1979) *Rev. Infect. Dis. 1*, 483.
Mollison, K. W., Fey, T. A., Krause, R. A., Mandecki, W., Fox, J. L., & Carter, G. W. (1987) *Agents Actions 21*, 366.
Müller, L., & Ernst, R. R. (1979) *Mol. Phys. 38*, 963.
Müller, N., Bodenhausen, G., Wüthrich, K., & Ernst, R. R. (1985) *J. Magn. Reson. 65*, 531.
Müller, N., Ernst, R. R., & Wüthrich, K. (1986) *J. Am. Chem. Soc. 108*, 6482.
Otting, G., Widmer, H., Wagner, G., & Wüthrich, K. (1986) *J. Magn. Reson. 66*, 187.
Pardi, A., Billeter, M., & Wüthrich, K. (1984) *J. Mol. Biol. 180*, 741.
Rance, M., Sørensen, O. W., Bodenhausen, G., Wagner, G., Ernst, R. R., & Wüthrich, K. (1983) *Biochem. Biophys. Res. Commun. 117*, 479.
States, D. J., Haberkorn, R. A., & Reuben, D. J. (1982) *J. Magn. Reson. 48*, 286.
Štrop, P., Wider, G., & Wüthrich, K. (1983) *J. Mol. Biol. 166*, 641.
Wagner, G. (1983a) *J. Magn. Reson. 55*, 151.
Wagner, G. (1983b) *Q. Rev. Biophys. 16*, 1.
Wagner, G., & Wüthrich, K (1982) *J. Mol. Biol. 155*, 347.
Wagner, G., & Zuiderweg, E. R. P. (1983) *Biochem. Biophys. Res. Commun. 113*, 854.
Wagner, G., Pardi, A., & Wüthrich, K. (1983) *J. Am. Chem. Soc. 105*, 5948.
Ward, P. A. (1970) *Arthritis Rheum. 13*, 181.
Weigle, W. D., Goodman, M. G., Morgan, E. L. & Hugli, T. E. (1983) *Springer Semin. Immunopathol. 6*, 173.
Wider, G., Macura, S., Anil Kumar, Ernst, R. R., & Wüthrich, K. (1984) *J. Magn. Reson. 56*, 207.
Williamson, M. P., Marion, D., & Wüthrich, K. (1984) *J. Mol. Biol. 173*, 341.
Williamson, M. P., Havel, T. F., & Wüthrich, K. (1985) *J. Mol. Biol. 182*, 295.
Wüthrich, K., Wider, G., Wagner, G., & Braun, W. (1982) *J. Mol. Biol. 155*, 311.
Wüthrich, K., Billeter, M., & Braun, W. (1984) *J. Mol. Biol. 180*, 715.
Zimmerman, B., & Vogt, W. (1984) *Hoppe-Seyler's Z. Physiol. Chem. 365*, 151.
Zuiderweg, E. R. P., Kaptein, R., & Wüthrich, K. (1983a) *Proc. Natl. Acad. Sci. U.S.A. 80*, 5837.
Zuiderweg, E. R. P., Kaptein, R., & Wüthrich, K. (1983b) *Eur. J. Biochem. 137*, 279.
Zuiderweg, E. R. P., Scheek, R. M., Boelens, R., van Gunsteren, W. F., & Kaptein, R. (1985) *Biochimie 67*, 707.
Zuiderweg, E. R. P., Hallenga, K., & Olejniczak, E. T. (1986) *J. Magn. Reson. 70*, 336.
Zuiderweg, E. R. P., Henkin, J., Mollison, K. W., Carter, G. W., & Greer, J. (1988) *Proteins: Struct., Funct., Genet.* (in press).